

# A New Shared Spectrum Access Paradigm between Cellular Wireless Communications and Radio Astronomy

H. Minn, *Fellow, IEEE*, Yahia R. Ramadan, *Student Member, IEEE*, and Yucheng Dai, *Student Member, IEEE*

**Abstract**—This paper proposes a new paradigm of shared spectrum access between cellular wireless communications (CWC) and radio astronomy systems (RAS). Traditionally, most spectrum chunks are separately allocated to CWC and RAS, with a few shared spectrum without guaranteed spectrum access for RAS. Furthermore, RAS sites are generally set up at remote locations, protected by radio quiet zones. In view of growths in spectrum demands from both systems, in population, and in applications and service deployments, the existing paradigm of geographical and spectral isolation between CWC and RAS will become inefficient. This paper develops a three phase spectrum access which enables geographical and spectral coexistence between CWC and RAS. Additionally, traffic statistics based improved spectrum access is developed. Furthermore, a built-in fine tuning mechanism is presented for addressing mismatches between design and practical environments as well as for facilitating service evolutions. Performance evaluation results demonstrate advantages of the proposed paradigm.

**Index Terms**—Spectrum utilization, Spectrum sharing, Cellular wireless, Radio astronomy, Three-phase spectrum access

## I. INTRODUCTION

Spectrum sharing has been viewed as an efficient approach for enhanced spectrum utilization. The obvious trend is that the active usage of the radio spectrum will rise substantially across time, frequency and space, which is much desirable from the spectrum utilization perspective but it could cause harmful radio frequency interference (RFI) to passive services such as radio astronomy and earth exploration remote sensing. These passive services provide economically and scientifically important observations of Earth's environment, our solar system and the cosmos [1]. Due to their benefits to society, several of the ITU-R recommendations stipulate for protection of them [2]–[7]. Thus, it is very crucial to develop new spectrum sharing paradigms between the active wireless communications and the passive remote sensing systems that answer the needs of both types of systems. This paper considers spectrum sharing scenarios between cellular wireless communications (CWC) and radio astronomy systems (RASs).

RASs make astronomical observations in all available atmospheric windows ranging from 2 MHz to 1000 GHz and above [2]. RASs are allocated with some dedicated primary bands and some secondary bands, but their spectral requirements continue to increase and some observations in the bands allocated to the active wireless services are essential for RAS [1]. In the past, sporadic spectrum use of active services allows RAS's observations in the active service bands during the unused time intervals. But such opportunities will diminish quickly as new wireless systems with dynamic spectrum access

proliferate. Furthermore, RFI detection (important task for RAS [8]–[14]) will become more challenging as commonly used non-Gaussianity test would become invalid for such emerging scenarios. To protect from RFI, RAS receivers are set up at remote locations and a radio quiet zone centered around each RAS receiver (additionally surrounded by a radio coordination zone) is imposed by regulation. In view of growths in population, active wireless services, and need of more RAS measurements and receivers, the existing approach of isolation of RAS receivers in remote locations together with radio protection zones [15], [16] would not be able to answer the future needs of the society, and new spectrum sharing strategies are in great need.

In this paper, we develop a new paradigm of spectrum sharing between CWC and RAS based on three-phase spectrum access which enables geographical and spectral coexistence between CWC and RAS. We present detailed design aspects, advanced resource allocation based on CWC's traffic statistics, and a built-in fine tuning feature to address design mismatches. Simulation study illustrates that the proposed approach can address the needs of CWC and RAS and provide substantially enhanced spectrum utilization.

## II. PROPOSED SHARED SPECTRUM ACCESS

The proposed shared spectrum access is based on the new paradigm of geographical coexistence between CWC and RAS systems with some form of guaranteed RFI-free spectrum access for RAS systems. We propose the following novel approaches to enable such coexistence paradigm. Their detailed design aspects will be described in the next section.

### 1. Three-Phase Time Division Spectrum Access:

We develop a shared spectrum access strategy based on the time division approach with three phases. Across time, each frame contains three phases, namely, CWC only phase, CWC+RAS phase, and RAS only phase. The three phases are repeated but the durations of the three phases can be time-dependent and different from repetition to repetition. They are predefined well in advance and known to both CWC and RAS.

During the CWC only phase, CWC transmits but RAS does not collect its data as it is heavily corrupted by RFI from CWC. RAS receivers are turned off to protect them from harmful RFI but auxiliary receivers (whose main purpose is to collect RFI and exploit it for performance enhancement) of RAS can do other tasks (e.g., RFI measurement). During the CWC+RAS phase, each CWC base station (BS) or its users can transmit during a phase-2 transmit interval (P2TI) which is BS-dependent and predefined. RAS can do RFI measurement, interference channel measurement, fine timing synchronization with CWC BSs, fine tuning of the shared spectrum access

This material is based upon work supported by the National Science Foundation under Grant No. 1547048. The authors are with the University of Texas at Dallas, Richardson, TX, USA. Contact E-mail: hlaing.minn@utdallas.edu.

zone (SSAZ) for future frames, and potentially its own data collection during RFI-free interval. During the RAS only phase, there is no CWC transmission within the SSAZ, thus RAS is free from CWC-induced RFI. RAS conducts reliable data collection during this phase.

2. *Three-Phase Time-Frequency Division Spectrum Access:* When multiple bands are shared, we devise a spectrum access strategy which follows the same three phase principle in each band but positions the frames of different bands in a way to minimize the physical layer latency of CWC. The design would also depend on the frequency spacing of the shared bands and the CWC's out-of-band spectrum characteristics.

3. *Adaptive Shared Spectrum Access:* As CWC traffic loads vary across time, we also propose to enhance the above three phase spectrum access strategies by using different modes of resource allocation between CWC and RAS at different hours of each day. Such adaptation modes and schedules are predefined well in advance based on the average traffic statistics across time. They can be adjusted over a larger time scale in response to service evolution of CWC under fair resource sharing between CWC and RAS.

4. *Built-in Fine Tuning for the Shared Spectrum Access:* We propose each RAS site has auxiliary receivers for measuring RFI coming from CWC. There exist some works [17]–[19] which use auxiliary receivers for RFI detection. But our approach offers enhanced utilization of the auxiliary receivers in that the proposed three phase access together with the auxiliary receivers provides a built-in fine tuning mechanism for addressing design mismatches of the shared spectrum access. Details will be discussed in Section IV.

### III. DESIGN STEPS

#### A. Shared Spectrum Access Zone (SSAZ)

**SSAZ with 1 RAS receiver:** An important step in developing the proposed shared spectrum access is to define a shared spectrum access zone (SSAZ) within which CWC and RAS follow the three phase spectrum access while CWC systems outside SSAZ can access their spectrum freely but their transmissions do not cause harmful RFI to RAS. For this, we adopt the interference power level threshold as defined in ITU-R RA.769-2 as the maximum RFI level the RAS receiver can tolerate and denote it by  $I_{th}$ . We consider downlink of CWC with full load to determine the RFI level at RAS. Suppose the SSAZ is with radius  $R$  meters centered at the RAS receiver, and the CWC hexagon cells, each with radius  $r$  meters, surround the RAS receiver as shown in Fig. 1. In calculating interference power experienced at RAS, we approximate each hexagonal cell by its inscribed circular cell with radius  $\sqrt{3}r/2$ . This yields closer CWC BSs to RAS than the hexagon case, thus giving an upper bound on the actual interference power and hence a safer design for RFI protection of RAS. The  $i$ th tier cell ring has  $K_i \triangleq \lceil \pi(2i-1) \rceil$  cells with the same distance  $d_i = (2i-1)\sqrt{3}r/2$  between BS and RAS receiver. Denote the BS of cell  $j$  at the  $i$ th tier cell ring by  $BS_{i,j}$ . Then, the SSAZ design based on  $S$  outer tiers can be given by

$$R = \min\{(2i_0 - 1)\sqrt{3}r/2\}, \quad (1)$$

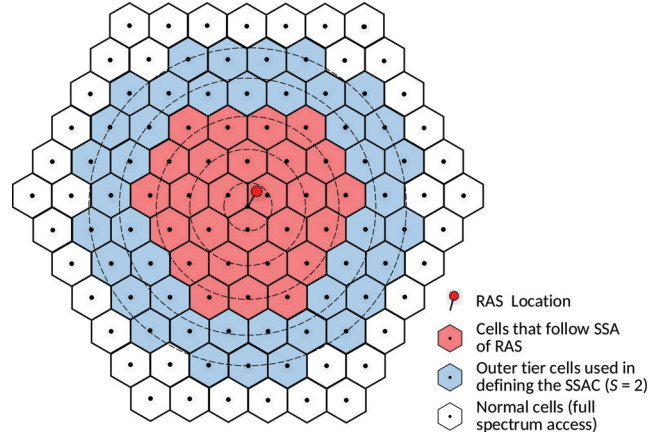


Fig. 1. Tiers of CWC cell rings around an RAS receiver

$$\text{s.t.} \quad \sum_{i=i_0+1}^{i_0+S} \sum_{j=1}^{K_i} P_{i,j} L(d_i) < I_{th},$$

where  $P_{i,j}$  is the effective radiated power of  $BS_{i,j}$ , and  $L(d_i)$  is the propagation path loss at the  $i$ th tier. Note that due to terrain constraints, associated path-loss and antenna down-tilting, using a finite  $S$  is justified. Fig. 1 illustrates the tiers of CWC hexagon cell rings around an RAS receiver, as well as the outer tiers ( $S = 2$  for presentation convenience) used in defining the SSAZ. In this illustration, the SSAZ is composed of 3 tiers (for presentation convenience) of CWC cells.

**SSAZ with  $M$  RAS receivers:** When there are  $M$  RAS receivers at different locations within a region of a potential SSAZ, the above design can be modified as follows. First, for each RAS receiver, we apply the above design as if there were only one RAS receiver. For RAS receiver  $m$ , we obtain the zone  $\widetilde{\text{SSAZ}}_m$  within which there are  $K_{in}^m$  BSs with the corresponding BS-to-RAS distances of  $\{d_{i,m}\}$ . Then, the final SSAZ(s) is (are) given by the union of all  $M$  zones as  $\{\text{SSAZ}_n\} = \cup_{m=1}^M \widetilde{\text{SSAZ}}_m$ . An illustration of a scenario with 3 RAS receivers is shown in Fig. 2 where  $\widetilde{\text{SSAZ}}_1$  and  $\widetilde{\text{SSAZ}}_2$  are combined into  $\text{SSAZ}_1$  while  $\widetilde{\text{SSAZ}}_3$  stands as  $\text{SSAZ}_2$ . Note that there are three groups of cells denoted by different colors within  $\text{SSAZ}_1$  due to how their P2TIs are computed (described in the next section).

#### B. Location-Dependent Three-Phase Frame Structure

After determining the SSAZ, the next step is to design the frame structure for the shared spectrum access. We address the CWC+RAS phase first. This phase absorbs propagation delays of different CWC BSs within the SSAZ so that those CWC signals do not arrive at the RAS receiver during the RAS only phase. This imposes a lower limit on the CWC+RAS phase duration  $T_{CWC+RAS}$ . Therefore, we have  $T_{CWC+RAS} > \kappa R / (3 \times 10^8)$ , where  $\kappa > 1$ , e.g.,  $\kappa = 2$ , to accommodate propagation model mismatches and RFI measurement/testing during the CWC+RAS phase.

To limit overhead due to the CWC+RAS phase,  $T_{CWC} + T_{RAS}$  should be substantially larger than  $T_{CWC+RAS}$ . On the other hand, if CWC requires minimum physical layer latency of  $\tau_{PHY}$ , then it requires  $T_{CWC+RAS} + T_{RAS} < \tau_{PHY}$ . Such

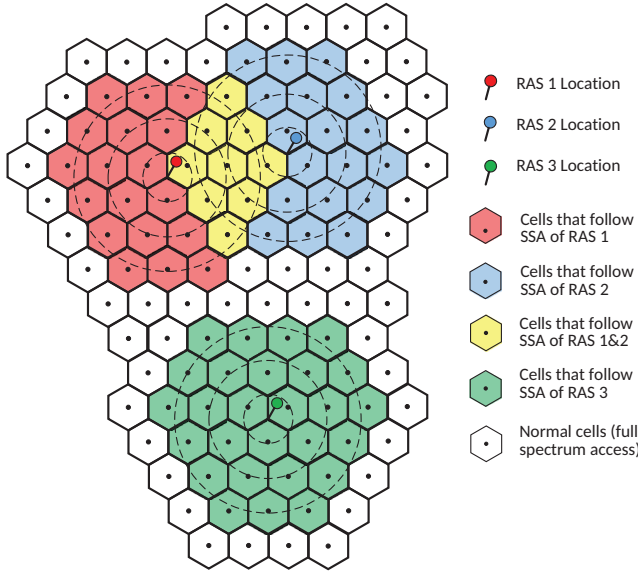


Fig. 2. An example scenario with 3 RAS sites and 2 SSAZs

latency constraint can be relaxed if there are other CWC-only resources or shared resources to support such QoS. The resource allocation between  $T_{CWC}$  and  $T_{RAS}$  could be set based on an agreed spectrum sharing policy.

We allow CWC BSs/users to transmit during their P2TIs provided their transmissions do not cause RFI during the RAS only phase. Let  $J_{SSAZ,i}$  denote the index set of SSAZs such that BS  $i$  is located within each of them and  $d_{i,m}$  represent the distance of BS  $i$  to  $\widetilde{SSAZ}_m$ ,  $m \in J_{SSAZ,i}$ . Without loss of generality, we will use OFDM since with a proper precoding it can also represent a single-carrier system. Let  $T_{sym}$  represent the OFDM symbol duration including the cyclic prefix interval. Then, we can design P2TI during the CWC+RAS phase for BS  $i$ , denoted by  $T_{ext,i,m}$  as

$$T_{ext,i} = \min_{m \in J_{SSAZ,i}} \left\lfloor \frac{T_{CWC+RAS} - d_{i,m}/(3 \times 10^8)}{T_{sym}} \right\rfloor T_{sym}. \quad (2)$$

The minimization in the above design avoids causing RFI to RAS when a BS is located within an overlapped region of two or more individual SSAZs. Note that different BSs in the same SSAZ have the same durations of the three phases but their P2TIs can be different depending on their locations.

### C. Design for Multiple Shared Bands

The design presented in the previous sections can be extended for multiple shared bands. As an example, we consider a scenario with two shared bands which are sufficiently separated in frequency such that CWC's transmission in one band does not cause RFI to the RAS's data collection in the other band. RAS receiver could operate in one of the two bands or in both bands, and for the latter case, it has capability of switching between the two bands electronically. Suppose the two shared bands have the same bandwidth, and CWC uses the same cell structure and the same OFDM system setting. Then, the SSAZ and the three phase frame structure will be the same as in the single shared band. Now, we introduce a frame time offset between the frames of the two bands such that the physical layer off duration of CWC is minimized. Fig. 3 illustrates the frame structures for the two shared bands. In

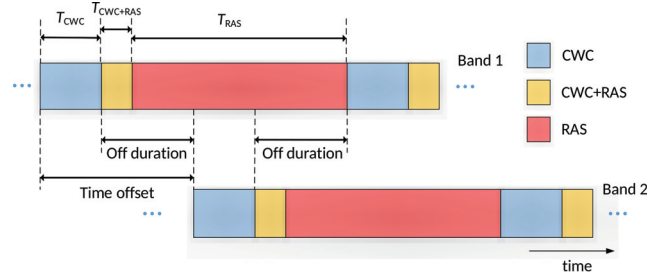


Fig. 3. Time-frequency division spectrum access for two shared bands

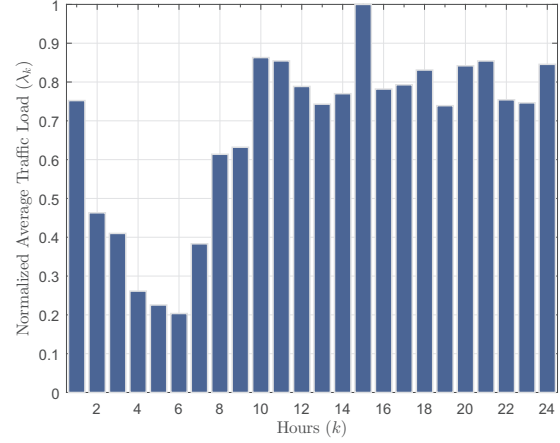


Fig. 4. Typical average normalized traffic load within a day

this case, with a time offset of half the frame duration, the physical layer off duration is reduced from  $T_{RAS} + T_{CWC+RAS}$  to  $\max([T_{RAS} + T_{CWC+RAS} - T_{CWC}]/2, 0)$ .

### D. Resource Adaptation based on Traffic Statistics

CWC wireless traffics show specific temporal usage characteristics and an example of such statistics within a day is shown in Fig. 4 [20]. Utilizing such traffic statistics, we propose to enhance the resource allocation through adaptation across time. Under the constraint that RAS must have a minimum resource amount in each frame and the ratio of the total resource amounts per day between CWC and RAS is maintained, we optimize the resource allocation across time to maximize CWC traffic support. Other optimization criteria are also possible but not considered here due to space limitation.

The frame structure at hour  $k$  can be defined by the three phases with durations  $T_{CWC,k}$ ,  $T_{CWC+RAS}$ , and  $T_{RAS,k}$ . Suppose one subframe duration  $T_{sf}$  is the minimum time unit that can be allocated among the three phases, and there are  $C$  resource blocks within  $T_{sf}$ . One frame duration  $T_f$  has  $n_f$  subframes. The numbers of subframes within  $T_{CWC,k}$ ,  $T_{CWC+RAS}$ , and  $T_{RAS,k}$  are  $n_{CWC,k}$ ,  $n_{CWC+RAS}$ , and  $n_{RAS,k}$  respectively, where  $n_{CWC,k} + n_{CWC+RAS} + n_{RAS,k} = n_f$  is the same across all hours. Note that the actual traffic load fluctuates and hence it can sometimes be much higher than the average traffic load during the considered hour. Suppose the CWC system is designed to support a maximum of  $n_{max,CWC}$   $C$  resource blocks per frame which is  $\alpha$  times the maximum average traffic load, e.g.,  $\alpha = 1.2$ . First, the average traffic loads per frame across 24 hours are scaled in units of resource blocks, e.g.,  $\lambda_k$  arrivals per frame, each requiring a

resource block, during hour  $k$ . Then, with  $\lambda_{\max} = \max_k(\lambda_k)$ , we have  $n_{\max, \text{CWC}} C = \alpha \lambda_{\max}$ . For illustration, the actual traffic per frame during hour  $k$  is modeled as a Poisson process with mean  $\lambda_k$ . Let  $F_{k,n}$  denote the probability that  $n$  resource blocks/frame are requested during hour  $k$ . Then, the CWC throughput per hour for hour  $k$ , denoted by  $\rho_k(n_{\text{CWC},k})$  or simply  $\rho_k$ , is defined as

$$\rho_k = \sum_{n=0}^{\infty} F_{k,n} \min(n, n_{\text{CWC},k} C). \quad (3)$$

Suppose CWC and RAS require a minimum of  $n_{\min, \text{CWC}}$  and  $n_{\min, \text{RAS}}$  subframes respectively in each frame, and the ratio of resource amounts per day between CWC and RAS during the CWC only and RAS only phases is  $\gamma$ . Then our resource allocation problem becomes designing the time-dependent frame structure to maximize the average CWC throughput as

$$\begin{aligned} \text{P1: } \{n_{\text{CWC},k}\} &= \arg \max_{\{n_{\text{CWC},k}\}} \sum_{k=1}^{24} \rho_k(n_{\text{CWC},k}), \\ \text{s.t. C1: } &\sum_{k=1}^{24} n_{\text{CWC},k} \leq N_{\text{CWC}}, \\ \text{C2: } &n_{\min, \text{CWC}} \leq n_{\text{CWC},k} \leq n_{\max, \text{CWC}}, \end{aligned} \quad (4)$$

where  $N_{\text{CWC}} = 24(n_f - n_{\text{CWC}+\text{RAS}})\gamma/(1+\gamma)$  and  $n_{\max, \text{CWC}} = n_f - n_{\text{CWC}+\text{RAS}} - n_{\min, \text{RAS}}$ .

The problem P1 is a nonlinear integer optimization problem, which is difficult to solve. Using the Gaussian approximation of a Poisson distribution, which is accurate for  $\lambda_k \geq 10$ ,  $\rho_k$  can be written as

$$\begin{aligned} \rho_k &= n_{\text{CWC},k} C - (n_{\text{CWC},k} C - \lambda_k) \Phi\left(\frac{n_{\text{CWC},k} C - \lambda_k}{\sqrt{\lambda_k}}\right) \\ &\quad - \sqrt{\frac{\lambda_k}{2\pi}} \exp\left(-\frac{1}{2\lambda_k} (n_{\text{CWC},k} C - \lambda_k)^2\right), \end{aligned} \quad (5)$$

where  $\Phi(\cdot)$  is the cumulative distribution function (CDF) of the standard normal distribution. We propose a successive resource allocation method which converges to the optimal solution of the integer-relaxed problem of P1.<sup>1</sup> Dropping C2, the Lagrangian function of the optimization problem P1 can be given by

$$\mathcal{L} = \sum_{k=1}^{24} \rho_k - \mu \left( \sum_{k=1}^{24} n_{\text{CWC},k} - N_{\text{CWC}} \right), \quad (6)$$

where  $\mu$  is the Lagrange multiplier. The Karush-Kuhn-Tucker (KKT) conditions are

$$\frac{\partial \mathcal{L}}{\partial n_{\text{CWC},k}} = C \left( 1 - \Phi\left(\frac{n_{\text{CWC},k} C - \lambda_k}{\sqrt{\lambda_k}}\right) \right) - \mu = 0, \quad (7)$$

$$\mu \left( \sum_{k=1}^{24} n_{\text{CWC},k} - N_{\text{CWC}} \right) = 0, \quad (8)$$

where  $\mu \geq 0$ . From (7), we get

$$\frac{n_{\text{CWC},k} C - \lambda_k}{\sqrt{\lambda_k}} = \frac{n_{\text{CWC},l} C - \lambda_l}{\sqrt{\lambda_l}}, \quad (9)$$

<sup>1</sup>The proof is similar to that of Proposition 2 in [21].

for  $k, l \in \{1, 2, \dots, 24\}$ . Using (8) and (9), we can solve the resource allocation problem P1 in a successive manner to satisfy C2 as illustrated in Algorithm 1. Generally, elements of  $\{n_{\text{CWC},k}\}_{k=J}^M$  obtained by Algorithm 1 are not integers. Thus, we proceed as follows. First, the quantity  $\Delta = N_{\text{CWC}} - \sum_{k=1}^{24} \lfloor n_{\text{CWC},k} \rfloor$  and the set  $\mathcal{D} = \{\lfloor n_{\text{CWC},k} \rfloor - n_{\text{CWC},k}\}_{k=J}^M$  are calculated. Next, we set  $n_{\text{CWC},k} = \lfloor n_{\text{CWC},k} \rfloor$  for  $k = J, J+1, \dots, M$ . Then, we distribute  $\Delta$  over as many elements of  $\{n_{\text{CWC},k}\}_{k=J}^M$  as possible by 1-unit increase according to the ascending order of  $\mathcal{D}$ . Then,  $\{n_{\text{CWC},k}\}$  is ordered according to the original order of  $\{\lambda_k\}$  (before sorting). Finally,  $n_{\text{RAS},k} = n_f - n_{\text{CWC}+\text{RAS}} - n_{\text{CWC},k}$  for  $k = 1, 2, \dots, 24$ .

---

#### Algorithm 1 Resource Allocation P1

---

**Input:**  $\{\lambda_k\}$ ,  $C$ ,  $n_{\min, \text{CWC}}$ ,  $n_{\max, \text{CWC}}$ ,  $N_{\text{CWC}}$

**Initial:**  $J = 1$ ,  $M = 24$ , flag = 1

- 1: **Sort**  $\{\lambda_k\}$  in ascending order
- 2: **while** flag **do**
- 3:  $n_{\text{CWC},J} = \frac{N_{\text{CWC}} - \sum_{k=J}^M \frac{1}{C} (\lambda_k - \sqrt{\lambda_k \lambda_J})}{\sum_{k=J}^M \sqrt{\frac{\lambda_k}{\lambda_J}}}$
- 4: **for**  $k = J + 1$  to  $M$  **do**
- 5:  $n_{\text{CWC},k} = \sqrt{\frac{\lambda_k}{\lambda_J}} n_{\text{CWC},J} + \frac{1}{C} (\lambda_k - \sqrt{\lambda_k \lambda_J})$
- 6: **end for**
- 7: flag = 0
- 8: **while**  $n_{\text{CWC},J} < n_{\min, \text{CWC}}$  **do**
- 9:  $n_{\text{CWC},J} = n_{\min, \text{CWC}}$
- 10:  $N_{\text{CWC}} = N_{\text{CWC}} - n_{\min, \text{CWC}}$
- 11:  $J = J + 1$
- 12: flag = 1
- 13: **end while**
- 14: **if not** flag **then**
- 15: **while**  $n_{\text{CWC},M} > n_{\max, \text{CWC}}$  **do**
- 16:  $n_{\text{CWC},M} = n_{\max, \text{CWC}}$
- 17:  $N_{\text{CWC}} = N_{\text{CWC}} - n_{\max, \text{CWC}}$
- 18:  $M = M - 1$
- 19: flag = 1
- 20: **end while**
- 21: **end if**
- 22: **end while**

**Output:**  $\{n_{\text{CWC},k}\}$ ,  $J$ ,  $M$

---

## IV. BUILT-IN FINE TUNING

RAS requires to have spectrum access without harmful RFI while CWC desires to have more spectrum access opportunities. The proposed approach facilitates them by means of the SSAZ and BS-dependent guard time intervals during the CWC+RAS phase. However, the channel conditions, the cell structures, and the wireless traffic statistics in practical environments may be different from those used in the design. Thus, meeting the system design goal (e.g., avoiding harmful RFI for RAS) is uncertain. For this critical practical issue, we propose a fine tuning mechanism which is a built-in characteristic of the proposed three phase spectrum access. During the initial deployment stage, the CWC+RAS phase is designed conservatively to avoid causing RFI to RAS in the RAS only phase. We also equip each RAS site with auxiliary receiver(s) which measures RFI from CWC. CWC and RAS coordinate for automatic fine tuning.

In the first phase of fine tuning, we adjust the SSAZ. Auxiliary receivers of RAS measure RFI from the CWC cells outside SSAZ during the CWC+RAS phase. If RFI level is below the acceptable threshold, increasing the SSAZ is not required. Otherwise, SSAZ should be increased by including the bordering outside tier of cells. This process is repeated until the RFI level falls below the acceptable threshold. If the RFI level is substantially lower than the threshold, we can remove CWC cells in the bordering inside tier from the SSAZ, one at a time, as long as the RFI level is below the threshold. BSs outside SSAZ do not share spectrum access with RAS, thus they have more spectrum access opportunities than the BSs within the SSAZ.

In the second phase of fine tuning, we adjust  $T_{\text{ext},i}$  for cells within SSAZ. BSs within SSAZ, one at a frame according to the predefined order, transmit during a few beginning symbols (duration less than initial  $T_{\text{ext},i}$ ) of the CWC+RAS phase, and the auxiliary receiver(s) at RAS measures RFI levels and their propagation delays. Then  $\{T_{\text{ext},i}\}$  are adjusted to be the largest integer multiple of  $T_{\text{sym}}$  such that CWC transmission during  $T_{\text{ext},i}$  at the beginning of the CWC+RAS phase does not cause RFI to the RAS only phase.

The above two phases of fine tuning just need to be done once at the initial deployment of the shared spectrum access. During that time, both CWC and RAS can operate in their respective CWC only phase and RAS only phase, thus, without any interruption of their normal operation. Due to service evolution, if new cell sites need to be added or the existing cells need to be re-structured (e.g., with different coverage zones), the fine tuning task can be invoked on a demand basis during the CWC+RAS phase. This provides a flexible coexistence between CWC and RAS while accommodating service evolutions of CWC and RAS.

Note that backbone communication between CWC and RAS is required for coordination but it would be infrequent and with low data rate. Furthermore, timing synchronization is required between CWC BSs and RAS receivers. For this, one can adopt an existing inter-BS synchronization scheme as used in TDD systems to avoid inter-cell interference between uplink and downlink. In fact, the fine tuning task also provides fine timing synchronization. For example, each BS can transmit known training signal during the fine tuning stage from which RAS can obtain the combined timing offset and propagation delay (e.g., [22]). Then RAS can provide feedback to CWC BSs through the backbone link to adjust their transmission time. Such fine timing synchronization can be implemented on a regular basis (e.g., once per day) or a need-basis.

## V. PERFORMANCE EVALUATION

In this section, we provide numerical results to analyze the proposed shared spectrum access paradigm between CWC and RAS. The simulation parameters are listed in Table I. Due to limited space, we limit our numerical results to SSAZ with a single RAS receiver and one shared band.

TABLE I  
SIMULATION PARAMETERS

Parameter	Value
Carrier frequency ( $f_c$ )	24 GHz
Bandwidth (BW)	500 MHz
Subcarrier spacing ( $\Delta f$ )	720 kHz
Symbol duration ( $T_{\text{sym}}$ )	1.604 $\mu\text{s}$
Cyclic prefix (CP)	215 ns
Subframe duration ( $T_{\text{sf}}$ )	38.5 $\mu\text{s}$
Frame duration ( $T_f$ )	1.694 ms
No. subframes / frame ( $n_f$ )	44
No. of resource blocks / subframe ( $C$ )	115
Min. RAS duration / frame ( $T_{\text{min,RAS}}$ )	0.4235 ms ( $n_{\text{min,RAS}} = 11$ )
Min. CWC duration / frame ( $T_{\text{min,CWC}}$ )	0.4235 ms ( $n_{\text{min,CWC}} = 11$ )
Traffic normalization constant ( $\alpha$ )	1.2
Ratio of resource amounts per day between CWC and RAS ( $\gamma$ )	5/4
Path loss model	mmWave model [23]
RAS interference threshold ( $I_{\text{th}}$ )	-195 dB ITU-R RA.769-2
RAS antenna radiation pattern	ITU-R SA.509-3 <sup>2</sup>
BS maximum transmit power ( $P_{\text{tx}}$ )	30 dBm
BS antenna radiation pattern	Omnidirectional
Cell radius ( $r$ )	200 m

We consider the millimeter wave (mmWave) path loss model in [23] and a total atmospheric absorption loss of 0.23 dB/km for frequency 24 GHz [24]. SSAZ is defined using (1) which yields an SSAZ with radius of 44.6 km (112 CWC tiers surrounding the RAS receiver). This distance requires a time duration of 148.67  $\mu\text{s}$  to absorb the propagation delays of different CWC BSs within the SSAZ. Therefore, we set  $T_{\text{CWC+RAS}} = 154 \mu\text{s}$ , i.e.,  $n_{\text{CWC+RAS}} = 4$  subframes.

As for maximizing the average CWC throughput, Fig. 5 shows the resource allocation during each hour. The resource amounts allocated to CWC approximately follow CWCs average traffic loads. At the hours with high traffic load, the resource amounts allocated to CWC are limited by  $n_{\text{max,CWC}}$ . At the hours with low traffic load, the resource amounts allocated to CWC are set to  $n_{\text{min,CWC}}$  to satisfy the latency requirement. Consequently, as shown in Fig. 6, CWC experiences reduced throughput at the hours with high traffic load which is expected due to allocation of a minimum of  $n_{\text{min,RAS}} = 11$  subframes per frame to RAS.

Fig. 7 shows the average spectrum utilization per hour defined as  $\eta_k = (\rho_k/C + n_{\text{RAS},k})/n_f$ . As expected, the proposed shared spectrum access yields average spectrum utilization of about 91% which is much larger than if the spectrum is allocated to CWC only.<sup>3</sup>

## VI. CONCLUSION

We have proposed a new paradigm of shared spectrum access between CWC and RAS by means of the three-phase spectrum access strategy. Shared spectrum access zones (SSAZs) are established around RAS sites. CWC systems within those zones follow the three-phase access while those outside SSAZ have full spectrum access. Both time-division and time-frequency division three-phase access schemes are presented. A built-in fine tuning mechanism is described for addressing design mismatches and service evolutions. Average

<sup>2</sup>The radio astronomy station almost receives the interference through the antenna side lobe (side lobe gain = -13 dB) [3]

<sup>3</sup>The above results have not included additional throughput improvement due to transmissions during  $T_{\text{ext},i}$  which varies from BS to BS.

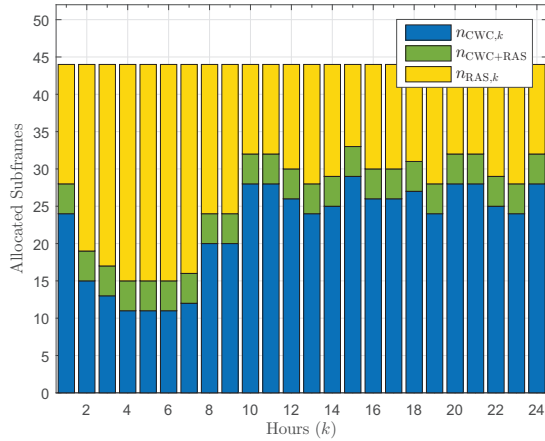


Fig. 5. Adaptive resource allocation for maximizing average throughput

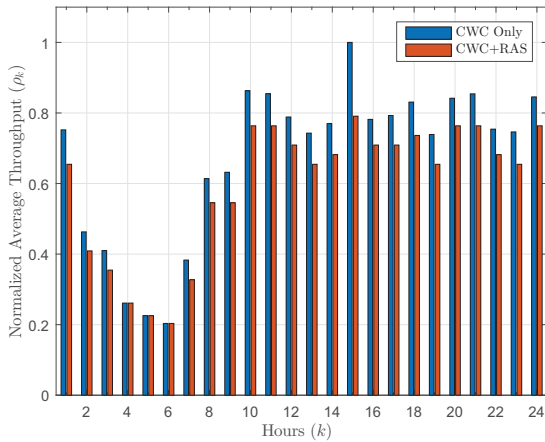


Fig. 6. CWC average throughput comparison between the CWC only allocation and the shared allocation

traffic pattern based resource allocation is further developed. The simulation results show that CWC systems within SSAZ experience slight throughput reduction at peak traffic hours but RAS achieves substantial RFI-free spectrum access which were infeasible in the existing paradigm. The overall spectrum utilization is also substantially enhanced, thus illustrating high potentials of the proposed paradigm.

## REFERENCES

- [1] *Spectrum Management for Science in the 21st Century*. Committee on Scientific Use of the Radio Spectrum, Committee on Radio Frequencies, and National Research Council, The National Academies Press, 2010.
- [2] ITU-R, "Preferred frequency bands for radio astronomical measurements," ITU, Recommendation RA.314-10, Jun. 2003.
- [3] —, "Space research earth station and radio astronomy reference antenna radiation pattern for use in interference calculations, including coordination procedures, for frequencies less than 30 GHz," ITU, Tech. Rep. SA.509-3, Dec. 2013.
- [4] —, "Protection criteria used for radio astronomical measurements," ITU, Recommendation RA.769-2, Mar. 2003.
- [5] —, "Levels of data loss to radio astronomy observations and percentage-of-time criteria resulting from degradation by interference for frequency bands allocated to the radio astronomy service on a primary basis," ITU, Recommendation RA.1513-2, Mar. 2015.
- [6] —, "Protection of the radio astronomy service in frequency bands shared with other services," ITU, Recommendation RA.1031-2, Jun. 2007.

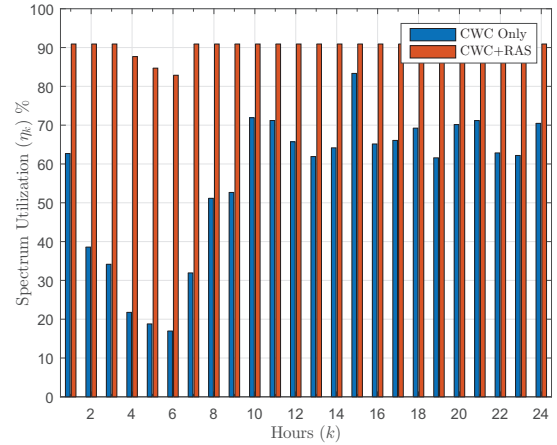


Fig. 7. Spectrum utilization comparison between the CWC only allocation and the shared allocation

- [7] A. R. Thompson, "ITU-R recommendations of particular importance to radio astronomy," in *Spectrum Management for Radio Astronomy*, vol. 1, 2004, p. 121.
- [8] ITU-R, "Techniques for mitigation of radio frequency interference in radio astronomy," ITU, Tech. Rep. RA.2126-1, Nov. 2013.
- [9] S. Misra and C. Ruf, "Analysis of radio frequency interference detection algorithms in the angular domain for SMOS," *IEEE Trans. Geosci. Remote Sens.*, vol. 50, no. 5, pp. 1448–1457, May 2012.
- [10] B. Guner, N. Niamsuwan, and J. Johnson, "Performance study of a cross-frequency detection algorithm for pulsed sinusoidal RFI in microwave radiometry," *IEEE Trans. Geosci. Remote Sens.*, vol. 48, no. 7, pp. 2899–2908, July 2010.
- [11] E. Njoku, P. Ashcroft, T. Chan, and L. Li, "Global survey and statistics of radio-frequency interference in AMSR-E land observations," *IEEE Trans. Geosci. Remote Sens.*, vol. 43, no. 5, pp. 938–947, May 2005.
- [12] F. Briggs and J. Kocz, "Overview of technical approaches to radio frequency interference mitigation," *Radio Science*, vol. 40, no. 5, 2005.
- [13] S. W. Ellington, "RFI mitigation and the SKA," *Experimental Astronomy*, vol. 17, no. 1-3, pp. 261–267, 2004.
- [14] A.-J. Boonstra, *Radio frequency interference mitigation in radio astronomy*. Dwingeloo, the Netherlands : ASTRON, 2005.
- [15] *Handbook of Frequency Allocations and Spectrum Protection for Scientific Uses*. NRC of the National Academies, The National Academies Press, 2007.
- [16] W. van Driel, "Radio quiet, please!- protecting radio astronomy from interference," in *IAU Symposium: The Role of Astronomy in Society and Culture*, vol. 260, 2009.
- [17] C. Barnbaum and R. F. Bradley, "A new approach to interference excision in radio astronomy: real-time adaptive cancellation," *The Astronomical Journal*, vol. 116, no. 5, p. 2598, 1998.
- [18] F. Briggs, J. Bell, and M. Kesteven, "Removing radio interference from contaminated astronomical spectra using an independent reference signal and closure relations," *The Astronomical Journal*, vol. 120, no. 6, p. 3351, 2000.
- [19] B. D. Jeffs, L. Li, and K. F. Warnick, "Auxiliary antenna-assisted interference mitigation for radio astronomy arrays," *IEEE Trans. Signal Process.*, vol. 53, no. 2, pp. 439–451, 2005.
- [20] X. Chen, Y. Jin, S. Qiang, W. Hu, and K. Jiang, "Analyzing and modeling spatio-temporal dependence of cellular traffic at city scale," in *IEEE Intl. Conf. Commun. (ICC)*, 2015.
- [21] N. Papandreou and T. Antonakopoulos, "Bit and power allocation in constrained multicarrier systems: the single-user case," *EURASIP J. Advances in Signal Processing*, vol. 2008, no. 1, pp. 1–14, 2007.
- [22] H. Minn, V. K. Bhargava, and K. B. Letaief, "A robust timing and frequency synchronization for OFDM systems," *IEEE Trans. Wireless Commun.*, vol. 2, no. 4, pp. 822–839, Jul. 2003.
- [23] M. K. Samimi, T. S. Rappaport, and G. R. MacCartney, "Probabilistic omnidirectional path loss models for millimeter-wave outdoor communications," *IEEE Wireless Commun. Lett.*, vol. 4, no. 4, pp. 357–360, 2015.
- [24] ITU-R, "Attenuation by atmospheric gases," ITU, Recommendation P.676-10, Sep. 2013.